

Numerical investigation of continuous hollow steel beam strengthened using CFRP

Amir Hamzeh Keykha*

Department of Civil Engineering, Zahedan Branch, Islamic Azad University, Zahedan, Iran

(Received May 31, 2017, Revised February 12, 2018, Accepted February 24, 2018)

Abstract. This paper presents a numerical study on the behavior of continuous hollow steel beam strengthened using carbon fiber reinforced polymers (CFRP). Most previous studies on the CFRP strengthening of steel beams have been carried out on the steel beams with simple boundary conditions. No independent study, to the researcher's knowledge, has studied on the CFRP strengthening of square hollow section (SHS) continuous steel beam. However, this study explored the effect of the use of adhesively bonded CFRP flexible sheets on the behavior of the continuous SHS steel beams. Finite Element Method (FEM) has been employed for modeling. Eleven specimens, ten of which were strengthened using CFRP sheets, were analyzed under different coverage length, the number of layers, and the location of CFRP composite. ANSYS software was used to analyze the SHS steel beams. The results showed that the coverage length, the number of layers, and the location of CFRP composite are effective in increasing the ultimate load capacity of the continuous SHS steel beams. Application of CFRP composite also caused the ductility increase some strengthened specimens.

Keywords: hollow continuous steel beam; CFRP strengthening; ultimate capacity; numerical investigation

1. Introduction

Nowadays, due to the increase of rebuilding costs in the worldwide, retrofitting and strengthening of existing structures seems necessary. Although the rebuilding cost is an important issue, but the preservation of heritage sites and ancient artifacts are more important than the rebuilding cost. Strengthening and retrofitting of steel structures is different. A practical and easy way for strengthening steel structures is the use of CFRP composite materials. The use of CFRP composite is a perfect solution to overcome on the shortcomings of existing steel structures which have been made in the past decades. In recent decades, some studies have been carried out on CFRP strengthening and retrofitting of the steel columns (Teng and Hu 2007, Bambach *et al.* 2009, Haedir and Zhao 2011, Fanggi and Ozbakkaloglu 2015, Ozbakkaloglu and Xie 2015, Kim and Harries 2011, Keykha *et al.* 2015, Keykha *et al.* 2016a, b). Some other studies have been done on flexural strengthening (Deng *et al.* 2004, Youssef 2006, Photiou *et al.* 2006), shear (Islam and Young 2013), tensile (Al-Zubaidy *et al.* 2013), and torsional of steel beams (Abdollahi Chakand 2013).

In another study, Sundarraja and Prabhu (2011) strengthened the hollow steel beams, which were first filled with concrete, using CFRP composite, and then they tested these specimens. The results showed that the strengthened specimens by full wrapping of CFRP composite exhibited more enhancements in stiffness and flexural moment capacity than other specimens. They also presented an

economical method for strengthening of the hollow steel beams that were filled with concrete.

Al Zand *et al.* (2015) strengthened the square CFST (concrete-filled steel tube) beams using the CFRP sheet. The results showed that for all strengthened CFST beams using one layer of CFRP sheet, CFRP had no significant enhancement in the ultimate load capacity when was wrapped along 50, 75 and 100% in length of the specimens. Keykha (2017a) carried out a numerical study to investigate the behavior of hollow steel frames. The steel frames were strengthened using CFRP composite on the beam bottom side and/or the location of connecting the beam to the column. The results showed that the coverage length and the number of layers of CFRP composite have a significant effect on increasing the ultimate load capacity of the hollow steel frames. Also, the results showed that the location of CFRP composite had no similar effect on increasing the ultimate load capacity and the mid-span deflection of the steel frames.

Moy (2007) strengthened the Acton Bridge on the London Underground system using CFRP plates. The Acton Bridge scheme showed the CFRP plate bonded to the tension flange of a steel beam has the effect on the bending stiffness of steel structures. To determine the bending stiffness, the steel I-beams strengthened by CFRP plates were also tested under cyclic loading. The results showed that the flexibility of the cured adhesive layer reduced the bending stiffness of the strengthened beam. The reduction in the bending stiffness of the strengthened steel I-beams was at most about 7%, while in the actual bridge was 4%.

Rizkalla *et al.* (2007) were applied a CFRP system for strengthening steel structures. They used from high modulus carbon fiber reinforced polymer (HM CFRP) materials for retrofitting of steel structures and bridges.

*Corresponding author, Ph.D.
E-mail: ah.keykha@iauzah.ac.ir

Table 1 Dimensions and properties of the SHS steel

Dimensions (h × b × s t) (mm)	Length L (mm)	Modulus of Elasticity (N/mm ²) Mean value	Stress (N/mm ²)	
			Yielding (F _y)	Ultimate (F _u)
100 × 100 × 5	2100	200000	280	340

Their study included selection of an appropriate adhesive for bonding HM CFRP materials as strengthening materials to steel and the large-scale steel-concrete composite beams. The results showed that the HM CFRP had a positive impact on the structural behavior of steel structures.

Keykha (2017b, c, d) investigated the SHS steel columns strengthened with the use of adhesively bonded CFRP flexible sheets under a combination of flexural moment and compression load. The results showed that the CFRP composite had no similar effect on the behavior of the slender and stocky SHS steel columns under the combined loads. The results also showed that the coverage length, the number of layers, and the location of CFRP composites had a significant effect on increasing the ultimate load capacity of the steel columns under the combined loads.

Awaludin and Sari (2015) carried out a numerical and experimental investigation on the nonlinear behavior of the SHS steel beams with simple boundary conditions. The investigated SHS steel beam in this research had an artificial crack (width 3 mm, depth 25 mm) at mid-span on tension side, and the SHS steel beams externally strengthened with CFRP sheet. Their studies showed that strengthen of the SHS steel beams having an artificial crack with CFRP sheets is a suitable solution of increasing the ultimate load capacity of these beams. In beam B (the strengthened beam by 1000 mm length of CFRP sheet at bottom surface), CFRP sheet was not very effective on the ultimate load capacity, due to the artificial crack was not completely covered with CFRP sheet. In beam C (the strengthened beam by 1000 mm length of CFRP sheet at bottom surface and both side faces of 25 mm depth), CFRP sheet was very effective on the ultimate load capacity, due to the artificial crack was completely covered with CFRP sheet.

Keykha (2017e, f, g) applied the CFRP sheets for strengthening steel members with initial deficiency to gain the ultimate load capacity. He carried out two schemes of strengthening for the steel members in both the longitudinal and transverse directions. The results showed that the impact of transverse deficiency on the ultimate load capacity of steel columns is higher than the longitudinal one. The results also showed that CFRP sheet can recover the ultimate load capacity of the steel members having a deficiency.

From the past studies, it is concluded that some studies have been carried out on the use of CFRP as a strengthening material for the SHS steel beams with simple boundary conditions. No independent article, to the researcher's knowledge, has existed in the field of CFRP strengthening of the continuous SHS steel beam. To fill the knowledge gap in this area, this study aims to investigate the effect of CFRP strengthening on the behavior of the continuous SHS steel beams, using numerical investigations. In this study to

Table 2 Properties of CFRP composite

CFRP Sheet: SikaWrap-230C				
Fabric design thickness (mm)	Modulus of Elasticity (N/mm ²)	Ultimate tensile strength (N/mm ²)	Ultimate tensile elongation (%)	Thickness (impregnated with Sikadur-330) (mm)
0.131	238000	4300	1.8	1

Table 3 Properties of adhesive

Adhesive: Sikadur-330			
Tensile strength (N/mm ²)	Modulus of Elasticity (N/mm ²)		Elongation at break (%)
	Tensile	Flexural	
30	4500	3800	0.9

investigate the behavior of the continuous SHS steel beams, the coverage length, the number of layers, and the location of CFRP composite were implemented.

2. Materials used

2.1 SHS steel

The SHS steel having a dimension of 100 mm × 100 mm was used in this study. The Length and thickness of the SHS steel were 2100 mm and 5 mm, respectively. The SHS steel had a yield stress of 280 N/mm², an ultimate stress of 340 N/mm², and the modulus of elasticity about 200000 N/mm² which were predicted from the experimental values (Keykha *et al.* 2015). The dimensions and material properties of the SHS steel used in this study are also given in Table 1.

2.2 CFRP composite

In this study, SikaWrap-230C is used. It is a unidirectional carbon fiber reinforced polymer with a nominal modulus of elasticity of 238000 N/mm², a nominal ultimate tensile strength of 4300 N/mm², and a nominal thickness of 0.131 mm that provided by the manufacturer. The properties of CFRP used in this research, SikaWrap-230C, is also shown in Table 2.

2.3 Adhesive

The used adhesive in this study is the Sikadur-330. This type of adhesive is a two-part system: a hardener and a resin. The mixing ratio is 1:4. The properties of used epoxy in this study are shown in Table 3.

3. Numerical simulation

3.1 Method description

To model the continuous SHS steel beams, the full 3D simulation using ANSYS software was performed. The continuous SHS steel beams, CFRP sheets and adhesive were simulated by using the 3D solid triangle elements (ten-nodes 187). Nonlinear static analysis was carried out to

Table 4 Comparison of the ultimate load of beams in both laboratory (Awaludin and Sari 2015) and numerical analysis

Model label	CFRP sheet (mm)	Experimental (kN)	FE analysis (kN)
Beam A	NA	10.93	11.01
Beam B	1000 × 100	13.17	14.12
Beam C	1000 × 150	20.87	21.30

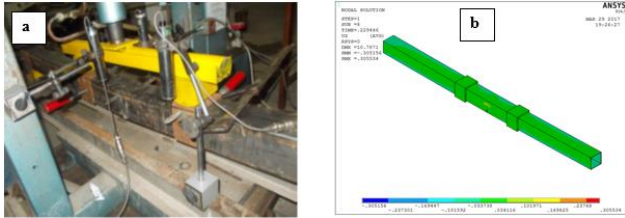


Fig. 1 Deformed shape of beam A. (a) Experimental (Awaludin and Sari 2015). (b) Numerical simulation

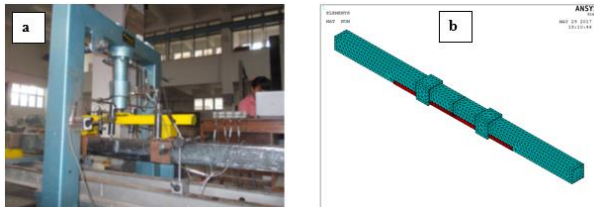


Fig. 2 The beam C. (a) under laboratory conditions (Awaludin and Sari 2015). (b) Numerical simulations

achieve the failures. In this case, the load was applied incrementally until the plastic strain in an element reached to its ultimate strain (element is killed). Linear and nonlinear properties of materials were defined. The material properties of the continuous SHS steel beams were defined as nonlinear materials. The properties of CFRP materials were defined as linear and orthotropic, because CFRP materials used in this study (SikaWrap-230C) have linear properties and they were unidirectional (Keykha 2017a). The adhesive was defined as the materials having linear properties. For meshing, the map meshing was used. Therefore, to analyze the specimens from the solid element of 187 with the mesh size of 25 was used (Keykha 2017a). These element and mesh size was used in the done study by Keykha (2017a) that the results of the analysis were satisfactory.

3.2 Validity of software results

It is necessary to validate the calculation of software. In this study, the software results have been validated and calibrated by the experimental results of Awaludin and Sari (2015). In numerical method, the beams loaded as in experimental (Awaludin and Sari 2015) and same boundary condition was analyzed (as shown in Figs. 1, 2). To analyze the specimens, the solid element of 187 with the mesh size of 25 was used. Fig. 3 shows the ultimate load-displacement curves of Beam A in both laboratory and numerical analysis. Table 4 also shows the ultimate load of the beam A, B and C in both laboratory (Awaludin and Sari 2015) and numerical analysis. These results show that there

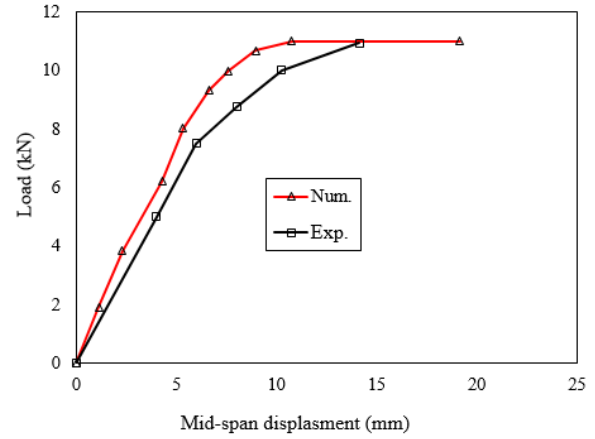


Fig. 3 Ultimate load-displacement curves of Beam A

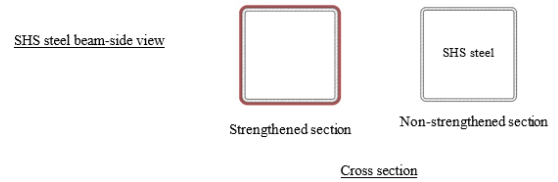
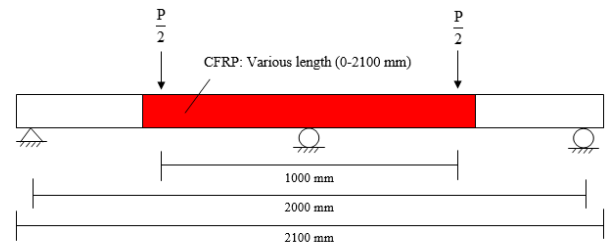


Fig. 4 Boundary conditions of the continuous SHS steel beam strengthened using CFRP

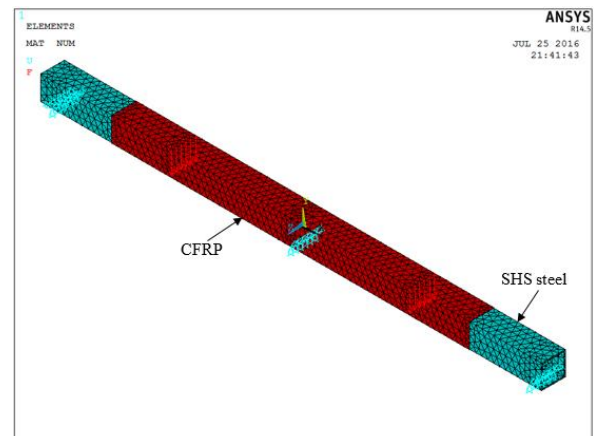


Fig. 5 Finite element modeling of specimen CB1-1500

is a good agreement between experimental and numerical values.

3.3 Model description

Nonlinear finite element models were prepared using ANSYS software to investigate the structural behavior of

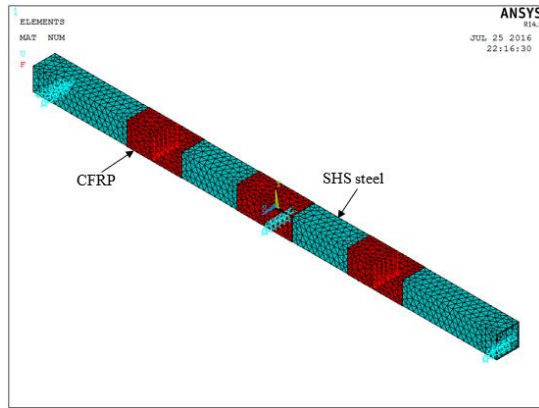


Fig. 6 Finite element modeling of specimen CB1-3-250

Table 5 Specimen details and analysis results

Designation of specimens	Number of layers CFRP	Length of CFRP coverage (mm)	Ultimate load (kN)	% of increase in ultimate load
CB0	0	0	166.80	0.00
CB1-500	1	500	181.73	8.95
CB2-500	2	500	200.98	20.49
CB1-1000	1	1000	187.33	12.31
CB2-1000	2	1000	220.34	32.10
CB1-1500	1	1500	203.84	22.21
CB2-1500	2	1500	264.35	58.48
CB1-2100	1	2100	207.02	24.11
CB2-2100	2	2100	267.04	60.10
CB1-3-250	1	3 × 250	212.65	27.49
CB2-3-250	2	3 × 250	243.27	45.85

the continuous SHS steel beams strengthened using CFRP sheets on four sides. All models were prepared as beams with simple supports, two-span in length, and two-point load applied at equal distance from each beam end. Fig. 4 shows the boundary conditions of the continuous SHS steel beams and strengthening scenario adopted in this study. For example, Figs. 5 and 6 also show three-dimensional finite element models of the prepared specimens using ANSYS software (specimen CB1-1500 and CB1-3-250). The applied pint loads were adopted in the finite element models. These loads gradually increased until the continuous SHS steel beams strengthened by CFRP sheets achieved their ultimate capacity.

3.4 Description of specimens

The analyzed continuous SHS steel beams include ten specimens strengthened with one and two CFRP layers. The CFRP sheets were applied on all four sides of the continuous SHS steel beams. To determine the increase rate in the ultimate load capacity of the continuous SHS steel beams strengthened using CFRP, one specimen was considered without CFRP strengthening (control specimen). To identify the specimen easily, the continuous SHS steel beams were designated by the names CB0, CB1-500, CB1-1000, CB1-1500, CB1-2100, CB1-3-250, CB2-500, CB2-1000, CB2-1500, CB2-2100, and CB2-3-250. For example,

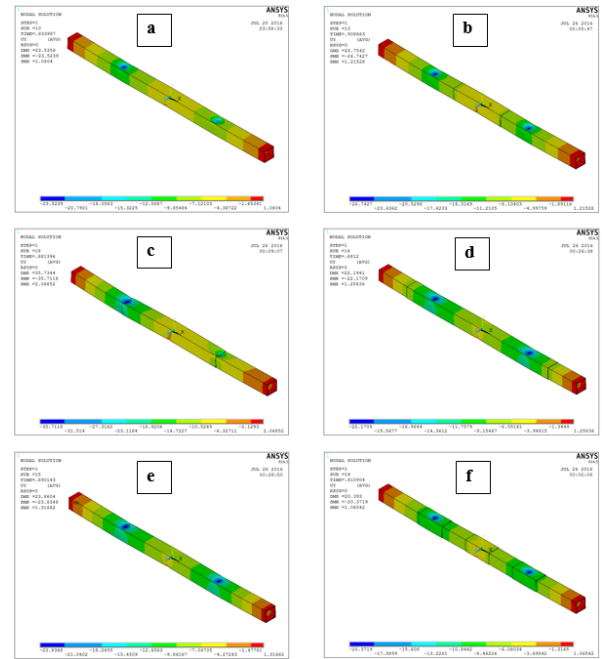


Fig. 7 Failure mode of the specimen. (a) CB0; (b) CB1-500; (c) CB2-1000; (d) CB2-1500; (e) CB2-2100; (f) CB2-3-250

the specimen CB2-1000 indicates that it is strengthened by two layers and 1000 mm CFRP length. The specimen CB1-3-250 specifies that it is the continuous SHS steel beam strengthened by one layer with 750 mm CFRP length in three positions. In this specimen, CFRP length in any position is 250 mm (see Fig. 6). Similarly, the specimen CB2-3-250 specifies that it is the continuous SHS steel beam strengthened by two layers with 750 mm CFRP length on four sides in three positions that the CFRP length in any position is 250 mm. The control specimen is named CB0 (the continuous SHS steel beams without CFRP strengthening).

4. Results and discussions

4.1 Ultimate load results of the specimens

Table 5 shows the numerical analysis results of the continuous SHS steel beams strengthened with one and two layers of CFRP sheet. The coverage length of CFRP varies based on the length of the continuous SHS steel beams. In the continuous SHS steel beams strengthened with the lengths of CFRP sheet 500-2100 mm, the center position of CFRP sheet is in the center of the continuous SHS steel beams on four sides. In specimen CB1-3-250 and CB2-3-250, the positions of CFRP location is such as shown in Fig. 6. The maximum ultimate load in the continuous SHS steel beams happened for the specimen CB2-2100. The percent of increase in the ultimate load capacity for this specimen was 60.10%.

4.2 Failure mode of the specimens

All specimens were subjected to two-point load on the top surface of the continuous SHS steel beams until failure.

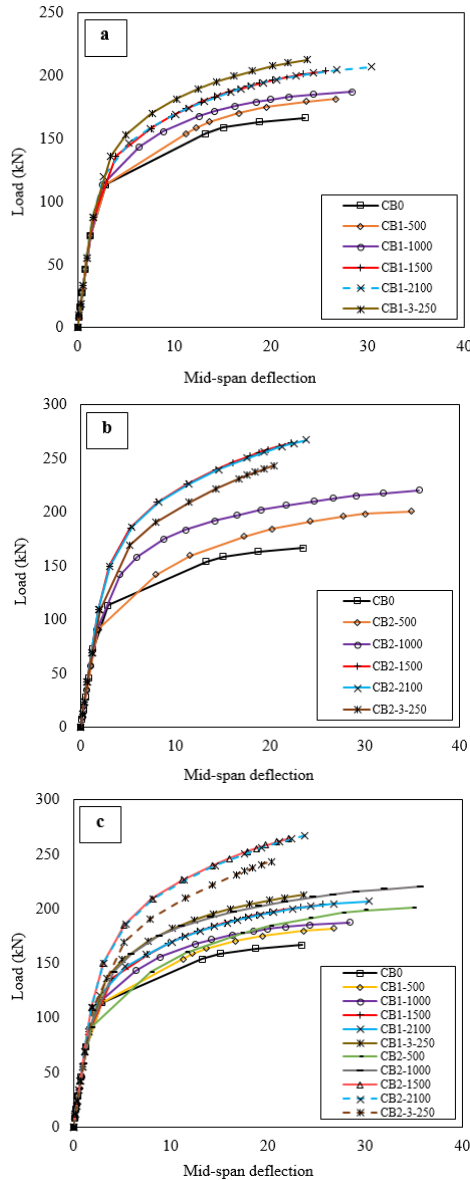


Fig. 8 Comparison of ultimate load–displacement curves. (a) Beams strengthened by one CFRP layer and non-strengthened beam. (b) Beams strengthened by two CFRP layers and non-strengthened beam. (c) All beams

Two local buckling at the top surface (in load under) of the continuous SHS steel beams were observed in the specimens CB0, CB1-500, CB1-1000, CB1-1500, CB1-2100, CB1-3-250, CB2-500, CB2-1000, CB2-1500, CB2-2100, and CB2-3-250 at the load of 166.80 kN, 181.73 kN, 187.33 kN, 203.84 kN, 207.02 kN, 212.65 kN, 200.98 kN, 220.34 kN, 264.35 kN, 267.04 kN, and 243.27 kN, respectively. The failure mode of all the continuous SHS steel beams was the same, so for example, the failure mode of six specimens is shown in Fig. 7.

4.3 Axial load-displacement behavior

The ultimate load capacity and the percent of increase in the ultimate load capacity of the continuous SHS steel beams, with respect to control specimen, were summarized

in Table 5. The ultimate load capacity-displacement curves were shown in Fig. 8(a)-(c). The control beam (control specimen) and the beams strengthened using CFRP sheet first exhibited the linear elastic behavior, then with an increase in loading, the behavior of the beams were the nonlinear inelastic (as shown in Fig. 8(a)-(c)). Furthermore, it is also observed that the strengthened beams tolerate higher load than the control beam. Fig. 8(c) shows that the greatest increase in the ultimate load capacity of the continuous SHS steel beams happens for the specimen CB2-2100. In this specimen, the number and the coverage length of CFRP layers are 2, 2100 mm (full coverage), respectively. Fig. 8(a) shows that the ultimate load capacity is almost equal for the specimen CB1-1500 and CB1-2100. Also, Fig. 8(b) shows that the ultimate load capacity is almost equal for the specimen CB2-1500 and CB2-2100. In these specimens (specimen CB1-1500 and CB1-2100; specimen CB2-1500 and CB2-2100), the ultimate load capacity-displacement curves are on each other (as shown in Fig. 8(a)-(c)).

4.4 Ductility capacity

The ductility capacity can be determined in different ways, such as by rotation, curvature and energy, displacement and so on. Feng *et al.* (2013) obtained the ductility capacity by deformation. They defined the ultimate deformation-to-the yielding deformation ratio as the ductility capacity. Fig. 8 shows that CFRP strengthening the continuous SHS steel beams using CFRP sheets improves the ductility capacity. In this study, the increase in the ductility capacity all specimens was observed, except in the specimen CB1-3-250 and CB2-3-250.

5. Conclusions

In this research, CFRP layers were applied with different coverage length on four sides of the continuous SHS steel beams to enhance their structural performance. Based on the obtained results, the failure modes, the ultimate load capacity, and the role of CFRP sheets on the behavior of the continuous SHS steel beams were discussed. Based on eleven analyzed specimens that ten specimens were strengthened with different coverage length and with one and two CFRP layers, the following conclusions were drawn:

- CFRP composite increased the ultimate load capacity of the continuous SHS steel beams. With an increase in the coverage length of CFRP sheet, the ultimate load capacity of the continuous SHS steel beams was increased. When the coverage length of CFRP sheet was more than 1500 mm, the ultimate load capacity was very little increased (compared the ultimate load capacity of specimen CB1-1500 and CB2-1500 with specimen CB1-2100 and CB2-2100).
- The number of layers and the coverage length of CFRP sheet had an impact on the percent of increase in the ultimate load capacity of the continuous SHS steel beams. The ultimate load capacity of the specimen CB1-3-250 was more than the ultimate load capacity other specimens

strengthened with one CFRP layer.

- The suitable coverage of CFRP sheet for strengthening the continuous SHS steel beams with two layers was full coverage (2100 mm length of CFRP sheet). The percentage of increase in the ultimate load capacity of this beam was 60.10% (see Table 5).

- The location of CFRP composite has a positive impact on increasing the ultimate load capacity of the continuous SHS steel beams. When the CFRP composite is located in under loads and/or, in the location of mid support of the continuous SHS steel beams, CFRP has a higher impact on the percent of increase of the ultimate load capacity (compared the ultimate load capacity of specimen CB1-500 until CB1-2100 with specimen CB1-3-250).

- The maximum ultimate load capacity of the continuous SHS steel beams strengthened with one and two layers CFRP happened for specimen CB1-3-250 and CB2-2100, and was 27.49% and 60.10 %, respectively.

- The increase in the ductility capacity all specimens strengthened using CFRP sheets was observed, except in the specimen CB1-3-250 and CB2-3-250.

It is significant to note that the results of this study were obtained based on the FE models, and in the future, it will need more experimental justification in this area.

References

- Abdollahi Chakand, N., Zamin Jumaat, M., Ramli Sulong, N.H., Zhao, X.L. and Mohammadzadeh, M.R. (2013), "Experimental and theoretical investigation on torsional behavior CFRP strengthened square hollow steel section", *Thin-Wall. Struct.*, **68**, 135-140.
- Al-Zubaidy, H., Al-Mahaidi, R. and Zhao, X.L. (2013), "Finite element modelling of CFRP/steel double strap joints subjected to dynamic tensile loadings", *Compos. Struct.*, **99**, 48-61.
- Al Zand, A.W., Badaruzzaman, W.H.W., Mutalib, A.A. and Qahtan, A.H. (2015), "Finite element analysis of square CFST beam strengthened by CFRP composite material", *Thin-Wall. Struct.*, **96**, 348-358.
- Awaludin, A. and Sari, D.P. (2015), "Numerical and experimental study on repaired steel beam using carbon fiber reinforced polymer", *Proceedings of the IABSE-ISCE Joint Conference on Advances in Bridge Engineering-III*, Dhaka, Bangladesh.
- Bambach, M.R., Jama, H.H. and Elchalakani, M. (2009), "Axial capacity and design of thin-walled steel SHS strengthened with CFRP", *Thin-Wall. Struct.*, **47**(10), 1112-1121.
- Deng, J., Lee, M.M.K. and Moy, S.S.J. (2004), "Stress analysis of steel beams reinforced with a bonded CFRP plate", *Compos. Struct.*, **65**(2), 205-215.
- Fanggi, B.A.L. and Ozbakkaloglu, T. (2015), "Square FRP-HSC-steel composite columns: Behavior under axial compression", *Eng. Struct.*, **92**, 156-171.
- Feng, P., Zhang, Y., Bai, Y. and Ye, L. (2013), "Strengthening of steel members in compression by mortar-filled FRP tubes", *Thin-Wall. Struct.*, **64**, 1-12.
- Haedir, J. and Zhao, X.L. (2011), "Design of short CFRP reinforced steel tubular columns", *J. Constr. Steel Res.*, **67**(3), 497-509.
- Islam, S.M.Z. and Young, B. (2013), "Strengthening of ferritic stainless steel tubular structural members using FRP subjected to two-flange-loading", *Thin-Wall. Struct.*, **62**, 179-190.
- Keykha, A.H. (2017a), "Numerical investigation on the behavior of SHS steel frames strengthened using CFRP", *Steel Compos. Struct.*, **24** (5), 561-568.
- Keykha, A.H. (2017c), "Effect of CFRP location on flexural and axial behavior of SHS steel columns strengthened using CFRP", *J. Struct. Constr. Eng.*, **4** (2), 33-46.
- Keykha, A.H. (2017d), "Numerical investigation of SHS steel beam-columns strengthened using CFRP composite", *Steel Compos. Struct.*, **25**(5), 593-601.
- Keykha, A.H. (2017e), "3D finite element analysis of deficient hollow steel beams strengthened using CFRP composite under torsional load", *Compos.: Mech. Comput. Appl.*, **8**(4), 287-297.
- Keykha, A.H. (2017f), "Structural behaviors of deficient steel members strengthened using CFRP composite subjected to torsional loading", *Proceedings of the 3th International Conference on Mechanics of Composites (MECHCOMP3)*, Bologna, Italy, July.
- Keykha, A.H. (2017g), "Finite element investigation on the structural behavior of deficient steel beam-columns strengthened using CFRP composite", *Proceedings of the 3th International Conference on Mechanics of Composites (MECHCOMP3)*, Bologna, Italy, July.
- Keykha, A.H. (2017b), "CFRP strengthening of steel columns subjected to eccentric compression loading", *Steel Compos. Struct.*, **23**(1), 87-94.
- Keykha, A.H., Nekooei, M. and Rahgozar, R. (2015), "Experimental and theoretical analysis of hollow steel columns strengthening by CFRP", *Civil Eng. Dimens.*, **17**(2), 101-107.
- Keykha, A.H., Nekooei, M. and Rahgozar, R. (2016a), "Analysis and strengthening of SHS steel columns using CFRP composite materials", *Compos.: Mech. Comput. Appl.*, **7**(4), 275-290.
- Keykha, A.H., Nekooei, M. and Rahgozar, R. (2016b), "Numerical and experimental investigation of hollow steel columns strengthened with carbon fiber reinforced polymer", *J. Struct. Constr. Eng.*, **3**(1), 49-58.
- Kim, Y.J. and Harries, K.A. (2011), "Behavior of tee-section bracing members retrofitted with CFRP strips subjected to axial compression", *Compos. Part B: Eng.*, **42**(4), 789-800.
- Moy, S. (2007), "CFRP reinforcement of steel beams adhesive cure under cyclic load", *Proceedings of the 1st Asia-Pacific Conference on FRP in Structures*, Hong Kong, December.
- Ozbakkaloglu, T. and Xie, T. (2015), "Behavior of steel fiber-reinforced high-strength concrete-filled FRP tube columns under axial compression", *Eng. Struct.*, **90**, 158-171.
- Photiou, N.K., Hollaway, L.C. and Chryssanthopoulos, M.K. (2006), "Strengthening of an artificially degraded steel beam utilising a carbon/glass composite system", *Constr. Build. Mater.*, **20**(1), 11-21.
- Rizkalla, S., Dawood, M. and Schnerch, D. (2007), "Development of a carbon fiber reinforced polymer system for strengthening steel structures", *Compos. Part A: Appl. Sci. Manufact.*, **39**(2), 388-397.
- Sundarraja, M.C. and Prabhu, G.G. (2011), "Finite element modelling of CFRP jacketed CFST members under flexural loading", *Thin-Wall. Struct.*, **49**(12), 1483-1491.
- Teng, J.G. and Hu, Y.M. (2007), "Behavior of FRP jacketed circular steel tubes and cylindrical shells under compression", *Constr. Build. Mater.*, **21**(4), 827-838.
- Youssef, M.A. (2006), "Analytical prediction of the linear and nonlinear behaviour of steel beams rehabilitated using FRP sheets", *Eng. Struct.*, **28**(6), 903-911.